FINAL TECHNICAL REPORT
February 1, 2006, through December 31, 2008

Project Title: **VALUE-ADDED PRODUCTS FROM FGD SULFITE-RICH SCRUBBER MATERIALS**

ICCI Project Number: DEV05-4
Principal Investigator: Vivak Malhotra, Southern Illinois University, Carbondale
Project Manager: Dr. Francois Botha, Illinois Clean Coal Institute

ABSTRACT

In this project, we explored a new strategy to find an effective utilization of sulfite-rich scrubber material, produced by wet flue gas desulfurization (FGD) scrubbers, by converting it into value-added wood-substitute composites. This was a cost share project, i.e., Illinois Clean Coal Institute provided cost share for the research being pursued under a US Department of Energy (National Energy Technology Laboratory) supported project.

The incoming scrubber materials were thoroughly characterized for their chemical and physical properties along with mercury's behavior in the sulfite-rich scrubber material at elevated pressures and temperatures. Our results suggested that at higher temperatures ($T < 275^{o}C$), pressure played an important role whether mercury would be re-emitted from the scrubber material during the fabrication of products. The results also indicated that the chemical structure of the sulfite-rich scrubber material remained invariant during the product development though hannebachite crystallites were flattened and more crystalline fines were generated. We successfully showed that it was feasible to produce two types of products, i.e., wood-substitute composites and load-bearing wood-substitute composites. We were able to generate materials, which had strength as high as 90 MPa (13,051 psi).

Pages 24 through 30 contain proprietary information.

EXECUTIVE SUMMARY

Objectives: The overall goal of this project was to develop technology which could effectively utilize FGD sulfite-rich scrubber material produced by power plants burning Midwestern high-sulfur coal. In pursuit of meeting the aforementioned goal, we were to establish whether it was feasible to fabricate value-added products such as wood-substitute products from sulfite-rich scrubber materials. In particular, the main objectives of our project were:

1. To thoroughly characterize, both physically and chemically, the sulfite-rich scrubber materials produced by a power plant located in Illinois which burns Illinois coal.
2. To evaluate the chemical stability of the scrubber products, especially under our material fabrication conditions.
3. To optimize the fabrication conditions for the development of wood substitute materials from sulfite-rich scrubber material.
4. To establish manufacturing conditions for the fabrication of load-bearing lumber material from sulfite-rich scrubber materials.
5. To evaluate the long-term stability of our products.
6. To generate technology transfer parameters so that products can move from laboratory to pilot-scale manufacturing.

Background: According to the American Coal Ash Association, about 29,250,000 tons of FGD byproducts were produced in the USA in the year 2003. Out of 29.25 million tons of FGD byproducts, 11.9 million tons were FGD gypsum byproduct. On the other hand, sulfite-rich scrubber byproduct's production was 17,350,000 tons in 2003. It is believed that about 70% of the total FGD gypsum produced is consumed in wallboard, Portland cement, and agricultural applications. The rest of the FGD gypsum, i.e., about 3.6 million tons is landfilled.

The economical and environmentally-conducive management of wet FGD sulfite-rich scrubber byproduct is much bleaker. Out of 17,350,000 tons of sulfite-rich scrubber material produced in 2003, only about 224,100 tons were used as structural fills/structural embankments and 259,608 tons for mining applications. The rest, i.e., 16,865,588 tons, was landfilled. Generally, wet FGD sulfite-rich scrubber material is stabilized or fixated by the addition of fly ash, cement, and/or lime prior to being landfilled. Unlike FGD gypsum, which when sold can garner resources for electric utilities, most power plants have to pay to dispose of sulfite-rich scrubber material. In fact, electric utilities paid to dispose of 2.08 million tons in 2000. Undoubtedly, the management problem is not only economical as the cost of landfilling continues to escalate but also may present environmental challenges for the long-term concerns associated with calcium sulfite landfills. Granted that in the near future most utilities are likely to install scrubber units which produce FGD gypsum, effective strategies are still required for managing the huge production of sulfite-rich scrubber material in the country. Clearly, environmentally-friendly and economically-conducive utilization of sulfite-rich scrubber material is of utmost importance for coal burning electric utilities. Our proposed research of developing wood-substitute products and synthetic lumber from sulfite-rich scrubber

materials and renewable byproducts precisely does that.

Experimental Approach: The sulfite-rich scrubber materials were procured from two different power plants, which burn high sulfur Midwestern coals. The wet scrubber cakes were subjected to drying analysis besides chemically and physically characterizing them with the help of XRD, DSC, TGA, DTA, and FTIR. We used a standard ASTM procedure to ascertain the mercury's behavior in the scrubber material prior to, during, and after our product manufacturing. We used compressive molding techniques to fabricate our wood-substitute composites from sulfite-rich scrubber materials. The fabricated composites were subjected to various ASTM procedures to evaluate the mechanical characteristics of our composites.

Results and Conclusions: In this cost-share project, we explored whether it was possible to develop wood-substitute products from FGD sulfite-rich scrubber material. To accomplish this, a range of characterization, mechanistic, and product development experiments was undertaken. The following summarizes the main findings of our project:

1. Gravimetric measurements suggested that water was rapidly lost at the ambient temperature from the scrubber cake for the first 24 hours, and thereafter there was a dramatic decrease in the rate of water evaporation. However, for our product manufacturing, 24 hours of scrubber cake drying would be adequate.
2. The physical structural analysis of the sulfite-rich scrubber material, obtained from two different power plants, indicated that the crystallites were typically hannebachite in appearance, i.e., platelet-like crystallites of $CaSO_3.0.5H_2O$. Our SEM measurements also revealed that the scrubber material from one of the power plants had a strong tendency to agglomerate in which crystallites stacked one over the other rather than forming spherical-looking agglomerates. The scrubber material from the second power plant did not show this behavior.
3. The XRD diffraction of the as-received, but air-dried, scrubber cake indicated peaks at 11.7, 16.1, and 16.7 degrees, thus, suggesting the scrubber cake to be a mixed phase of $CaSO_3.0.5H_2O$, $CaSO_3.4H_2O$, and $(CaSO_4)_x.(CaSO_3)_{1-x}.nH_2O$.
4. Our DSC measurements indicated that the products developed from the sulfite-rich scrubber materials would be stable as long as the temperature was $< 400^oC$.
5. Our results indicated that the mercury concentrations in sulfite-rich scrubber material should be determined at least after 14 days of air drying ($T < 30^oC$) time because of continued water loss from the scrubber material.
6. On subjecting the scrubber material to high temperatures and pressures typically expected during our product development, we did not observe any statistically significant emission of mercury from the scrubber cake.
7. The detailed thermal measurements, i.e., TGA and DTA analyses at $50^oC \leq T \leq 1250^oC$, on the scrubber materials suggested that there are four main thermal events by which scrubber material from both power plants decomposed. Consistent with the DSC results, TGA and DTA measurements also reinforced our suggestion that in our wood-substitute composites, the scrubber material would not decompose at $T < 400^oC$. Above 400^oC, half a water molecule was lost from the hannebachite crystallites, thus this might retard the flammability of our composites.

8. The exposure of sulfite-rich scrubber material to high-pressure (ambient pressure ≤ P < 3000 psi) and high-temperature (25^{o}C < T < 250^{o}C) resulted in the compression of hannebachite crystallites though they maintained their platelet-like shape. However, it was noticed that higher pressures, i.e., P > 1100 psi, and higher-temperatures, i.e., T > 200^{o}C, generated a considerable number of fines. The production of these fines during composite fabrication conditions could result in higher densities of the material. The vibrational (infrared) analysis of the scrubber materials, which were subjected to high-temperatures at high-pressure, indicated that the sulfite-rich scrubber materials retained their chemical structure under the above-mentioned conditions.
9. Our results showed that it was feasible to make composite materials from FGD sulfite-rich scrubber material with flexural strengths up to 90 MPa (13,050 psi). Formation pressure and temperature played an important role, besides the ingredients, in determining the final strength and elastic properties.
10. Depending upon the type of polymer, it appeared that wood-substitute composites could be formulated with sulfite-rich scrubber material with a concentration ranging from 60 wt% to 75 wt%. It also appears that the density of the composites derived from sulfite-rich scrubber material could be lowered either by the addition of fly ash or hollow spherical particles. However, hollow spherical particles were more effective in lowering the density yet maintaining the higher strength.
11. Our results suggest that post-curing the wood substitute composites developed from sulfite-rich scrubber material resulted in defect sites and micropores. This effectively reduced the density slightly though the strength of the composite also decreased by about 4 MPa. Therefore, it is recommended that wood-substitute composites fabricated from scrubber material not be subjected to post-curing.
12. We demonstrated that by combining recycled thermoplastics obtained from consumer recycled products with scrubber materials load-bearing wood plastic composites could be formulated. Flexural strengths in the range of 15 MPa – 30 MPa were achieved, which is comparable to other engineered-wood composites. Storage modulus at sub-ambient temperatures was improved with the addition of calcium sulfite into recycled thermoplastic.

Pages 24 through 30 contain proprietary information.

OBJECTIVES

The overall goal of this project was to develop technology which could effectively utilize FGD sulfite-rich scrubber material produced by power plants burning Midwestern high-sulfur coal. In pursuit of meeting the aforementioned goal, we were to establish whether it was feasible to fabricate value-added products such as wood-substitute products from sulfite-rich scrubber materials. In particular, the main objectives of our project were:

7. To thoroughly characterize, both physically and chemically, the sulfite-rich scrubber materials produced by a power plant located in Illinois which burns Illinois coal.
8. To evaluate the chemical stability of the scrubber products, especially under our material fabrication conditions.
9. To optimize the fabrication conditions for the development of wood substitute materials from sulfite-rich scrubber material.
10. To establish manufacturing conditions for the fabrication of load-bearing lumber material from sulfite-rich scrubber materials.
11. To evaluate the long-term stability of our products.
12. To generate technology transfer parameters so that products can move from laboratory to pilot-scale manufacturing.

INTRODUCTION AND BACKGROUND

According to the American Coal Ash Association, about 29,250,000 tons of FGD byproducts were produced in the USA in the year 2003. Out of 29.25 million tons of FGD byproducts, 11.9 million tons were FGD gypsum byproduct. On the other hand, sulfite-rich scrubber byproduct's production was 17,350,000 tons in 2003. It is believed that about 70% of the total FGD gypsum produced is consumed in wallboard, Portland cement, and agricultural applications. The rest of the FGD gypsum, i.e., about 3.6 million tons is landfilled.

The economical and environmentally-conducive management of wet FGD sulfite-rich scrubber byproduct is much bleaker. Out of 17,350,000 tons of sulfite-rich scrubber material produced in 2003, only about 224,100 tons were used as structural fills/structural embankments and 259,608 tons for mining applications. The rest, i.e., 16,865,588 tons, was landfilled. Generally, wet FGD sulfite-rich scrubber material is stabilized or fixated by the addition of fly ash, cement, and/or lime prior to being landfilled. Unlike FGD gypsum, which when sold can garner resources for electric utilities, most power plants have to pay to dispose of sulfite-rich scrubber material. In fact, electric utilities paid to dispose of 2.08 million tons in 2000. Undoubtedly, the management problem is not only economical as the cost of landfilling continues to escalate but also may present environmental challenges for the long-term concerns associated with calcium sulfite landfills. Granted that in the near future most utilities are likely to install scrubber units which produce FGD gypsum, effective strategies are still required for managing the huge production of sulfite-rich scrubber material in the country. Clearly, environmentally-friendly and economically-conducive utilization of sulfite-rich scrubber material is of utmost importance for coal burning electric utilities. Our proposed research of

developing wood-substitute products and synthetic lumber from sulfite-rich scrubber materials and renewable byproducts precisely does that.

EXPERIMENTAL PROCEDURES

Sulfite-Rich Scrubber Material:

The sulfite-rich scrubber material was provided by a power plant located in Illinois, which burns high-sulfur Illinois bituminous coal {henceforth called Power Plant A (PPA)}. The scrubber materials were in wet cake form and were collected throughout the life of this project. A second source of the wet scrubber material was from a power plant located in Indiana {Power Plant B (PPB)} which also burns high sulfur Midwestern coal.

TASK 1: Infrared (IR) Measurements:

The IR spectrum of the scrubber material was obtained using a Thermo Electron 670 Fourier transform infrared (FTIR) spectrometer equipped with a KBr beam splitter and a DTGS detector. We did not use the conventional KBr pellet approach to record our IR spectra because our past experience suggests that during KBr pellet formation, under high pressure, there is a potential of chemical reaction between KBr and $CaSO_3$. Instead, we formed mulls by hand grinding the scrubber material with mineral oil. The sample mulls were smeared between two KBr window optical flats, and the samples' spectra were recorded by acquiring 50 scans at 4 cm^{-1} resolution.

TASK 1: Mercury Analysis:

We used EPA 7473 method to analyze the mercury concentration in the scrubber materials. A commercial mercury analyzer, i.e., DMA-80 (Milestone, Inc.), was used for this purpose. The scrubber materials were air-dried in cleaned dishes for various lengths of time before subjecting the samples to Hg analysis. The air-dried samples were weighed (approximately 0.4 g) and loaded in nickel boats. The DMA-80 equipment consists of a thermal decomposition chamber followed by a catalytic conversion chamber, gold amalgamation system, and an atomic absorbance spectrophotometer. Controlled heating is used to first dry and then thermally decompose a sample in a quartz decomposition tube. A continuous flow of oxygen carries the decomposition products through a heated catalytic bed where SO_2, N_2, and halogens are trapped. All mercury species are reduced to Hg^0 and are carried over to the gold amalgamator where mercury is selectively trapped. The non-mercury vapors and decomposition products are flushed from the system prior to rapidly heating the gold amalgamator. The rapid heating of the amalgamator releases the mercury vapor, and the released vapors are subjected to a single beam, fixed wavelength (253.7 nm) atomic absorbance spectrophotometer. The output data are displayed as ng/g or as μg/kg of mercury concentration.

For our samples, we used the drying temperature of 300^{o}C and decomposition temperature of 800^{o}C. For the results reproduced in this report, we ran each sample at least four to five times to ensure a representative concentration of Hg in the sample. The blank boats were run intermediately between sample runs to eliminate any mercury memory effects. This approach, i.e., running blank sample boats between sample runs, provided an additional check for AA spectrophotometer's ability to accurately measure

mercury concentrations. To clean our sample boats, we first removed ash from the boats by simply wiping them. The wiped boats were then ultrasonically cleaned in distilled water for 2 to 3 hours. The ultrasonic cleaning was followed by heating the nickel boats in a furnace to 850^{o}C to ensure the removal of residual Hg. Between run days, the standard sample of apple leaves (Standard 1515) obtained from the National Institute of Standards and Technology (NIST) was run to ensure the accuracy of the system at low mercury concentration levels.

It is known that most scrubber units facilitate the capture of mercury, especially water soluble oxidized mercury while scrubbing SO_2. Because our composites were to be formulated at higher temperatures, i.e., 140^{o}C < T < 230^{o}C, and at higher pressures, i.e., P > 30 psi, there was a concern whether mercury captured by the scrubber materials could be re-emitted. As mentioned above, the mercury analysis of sulfite-rich scrubber was performed on the air-dried material. However, to determine whether any mercury would be re-emitted during our product manufacturing conditions, we prepared samples by hot-pressing pure scrubber material in a high pressure stainless steel die, simulating actual sample fabrication conditions. First, the temperature series was performed by preparing samples under 1000 psi (7 MPa) pressure at 140^{o}C, 155^{o}C, 170^{o}C, 185^{o}C, 200^{o}C, 215^{o}C, 230^{o}C, and 245^{o}C. Then, the point corresponding to an onset of change in mercury behavior was picked to perform a pressure series where samples were prepared using fabrication pressures from 0 psi to 11000 psi.

TASK 2: Scanning Electron Microscopy (SEM):
The crystalline behavior of the as-received sulfite-rich scrubber materials from Power Plants A was ascertained by obtaining their microscopic picture, using SEM technique. We used a Hitachi S570 scanning electron microscope to record our pictures.

TASK 3: Differential Scanning Calorimetry (DSC) Measurements:
The thermal behavior of as-received scrubber material was ascertained by subjecting it to DSC measurements at 30°C < T < 500°C. The DSC data were acquired on a Perkin-Elmer DSC7 system, interfaced with a PC computer using a Pyris (Perkin-Elmer) software. The DSC was calibrated for temperature and enthalpy. The temperature calibration was performed by the two-point method, using the melting transitions of indium (157°C) and zinc (420°C). The accuracy in temperature between 30°C and 420°C, based on our calibration procedure, was estimated to be ±1°C. The enthalpy calibration was performed using indium heat of fusion as the standard. After the enthalpy calibration, the DSC data on zinc metal were re-recorded, and the observed enthalpy of the melting transition of zinc was consistent with the values reported in the literature. The conditions under which the instrument calibration was performed exactly matched the experimental run conditions, namely the scan rate of 10°C/min, oxygen gas purge at 30 psi pressure. Also, during both calibration and heating runs, the dry box assembly over the sample head was flushed with nitrogen gas to maintain thermodynamic equilibrium. Aluminum (Al) sample pans in an unsealed mode generally were used to determine the thermal behavior of the scrubber materials. This was achieved by pushing down the top sample pan cover gently onto the bottom pan containing the sample.

TASK 3: Thermal Gravimetric Analysis (TGA) and Differential Thermal Analyzer (DTA) Measurements:
The high temperature thermal stability of the sulfite-rich scrubber materials was evaluated by subjecting the scrubber materials to TGA and DTA measurements at $50^{o}C \leq T \leq 1200^{o}C$. Both TGA and DTA curves were obtained under nitrogen gas environment. We used Perkin-Elmer's Diamond TGA system to record gravimetric curves.

The high temperature thermal behavior of sulfite-rich scrubber sludges was probed using a Perkin-Elmer DTA7 system capable of operating at $50^{o}C < T < 1650^{o}C$. This DTA equipment is capable of operating under various gas environments. A heating rate of $10^{o}C\ min^{-1}$ was used. We used α-Al_2O_3 powder as a reference material for our experiments.

TASKS 5, 6, and 7: Materials and Composite Fabrication Procedures*:*
Sulfite-rich scrubber material was air dried for at least 24 hours prior to analysis and composite fabrication. Agricultural crop byproducts were used as additive material for our products. Crop material was first ground with a large scale hammer mill to obtain particle size of ~ 2 to 3 cm in length, and this material was further ground in a cyclone mill to obtain micron-sized particles. The crop materials used for our composite manufacturing were largely composed of cellulose (40 – 60 %), hemicelluloses (20 – 40 %), and lignin (10 – 25 %). For the additive material, we used three different crops which have a slightly different cellulose-hemicellulose-lignin ratio. In general, these crop materials are very cheap and are readily available in the USA.

We used scrubber material obtained from PPA and crop materials obtained from Illinois sources for our composite fabrication. Even though by using high pressures and temperatures the composites could be fabricated purely from these two components, it was believed that the addition of a small amount of additives could greatly enhance the mechanical properties of the final product. Therefore, we tested various synthetic polymers in small quantities. The scrubber material along with crop byproducts and additives were mixed in a high-speed, high-shear blender prior to adding the ingredients in a high-pressure, high-temperature stainless steel die. The die was hot pressed at the predetermined temperature and pressure. During the hot pressing, gases were produced and the pressure was bumped to ensure that gases escaped into our venting system. After hot-pressing, the samples were ejected from the stainless steel die and were subjected to mechanical testing.

TASKS 8 and 12: Mechanical Testing:
The composites were cut into rectangular strips measuring approximately 4 mm x 6 mm x 50 mm and were then subjected to mechanical testing. The flexural strength of the composites was determined with the help of a commercial (ELE International) universal testing machine equipped with an in-house built three point bending fixture. The sample was placed on two parallel stainless steel pins, and the load was applied in the middle. The applied load was increased at a constant rate. The loading nose was attached to the load cell which precisely measured the pressure applied to the sample. The linear vertical displacement sensor values were used to determine the strain that the sample sustained

during the measurement. Flexural strength was determined according to ASTM D790 standard method, which is a maximum sustained stress by the sample at break and was calculated using the following equation:

$$\sigma = \frac{3Fl}{2bh^2},$$

where F, l, b, and h are the load at failure, span length, width, and thickness, respectively. Strain values were determined from the displacement data:

$$r = \frac{6Dd}{L^2},$$

where D is the mid-span deflection, d is the depth of the beam, and L is the support span. Load and displacement data were used to generate stress vs. strain curves.

RESULTS AND DISCUSSION

TASK 1. Chemical Analysis:

The as-received sulfite-rich scrubber materials from PPA and PPB were sent to a commercial laboratory for chemical analysis. The scrubber material was air-dried for more than a week at ambient temperature prior to sending the samples for analysis. Table 1 lists the concentrations of chlorine (Cl), arsenic (As), selenium (Se), boron (B), and cadmium (Cd) in the scrubber material from both power plants. It should be noticed from Table 1 that the chlorine content of Power Plant B's scrubber material was much higher than for the scrubber material from Power Plant A. Moreover, it appeared that the scrubber material from Power Plant B had higher selenium and boron content than that for Power Plant A.

Table 1. Chemical analysis of as-received but air-dried sulfite-rich scrubber materials.

Chemical	Power Plant A (PPA)	Power Plant B (PPB)
Chlorine (as-received)	0.01%	0.16%
Chlorine (dry)	0.01%	0.16%
Arsenic (As)	< 1 mg/g	< 1 mg/g
Selenium (Se)	< 1 mg/kg	< 4 mg/kg
Boron (B)	20 mg/g	127 mg/g
Cadmium (Cd)	< 1 mg/kg	< 1 mg/kg

TASK 2. Bulk Densities and X-ray Analysis:

We measured the apparent bulk density of the PPA scrubber material at 689 kg/m^3, while the Crop A material had an apparent density of 215 kg/m^3. High fabrication pressures, however, may greatly increase the density of composites.

Figure 1 shows the X-ray diffraction patterns observed for air-dried sulfite-rich scrubber

material for PPB. It should be noted that the scrubber material had not undergone fixation, thus, the material is not expected to contain fly ash particles unless the particles are due to impurities. In the 2θ range of 5 to 65°, the main diffraction d-spacing was observed at 7.6, 5.5, 5.3, 4.3, 4.25, 3.78, 3.15, 3.07, 2.67, and 4.25 Å. The main d-spacing for $CaSO_3.0.5H_2O$ (in the order of descending intensity) was at 3.16, 2.63, and 5.56 Å, while for $CaSO_3.4H_2O$ crystals the d-spacing match with 5.74, 3.62, and 2.67 Å. The major reflections observed for gypsum ($CaSO_4.2H_2O$) are at 7.56, 4.27, 3.06, 2.87, and 2.68 Å. The reflections observed at 7.6, 4.25, and 3.07 Å did suggest the presence of $CaSO_4.2H_2O$ in the scrubber material; however, as reported by Gadalla and Gupta [1], it is more likely that sulfate exists in a solid solution in the form $(CaSO_4)_n(CaSO_3)_{1-n}.XH_2O$. The observed diffraction patterns of sulfite-rich scrubber material, as expected, did indicate the presence of $CaSO_3.XH_2O$. However, based on the observed d-spacing values, we could not discount either $CaSO_3.0.5H_2O$ or $CaSO_3.4H_2O$ crystalline phase in the scrubber material. It is more likely that both hydrated sulfite phases are present in the scrubber material.

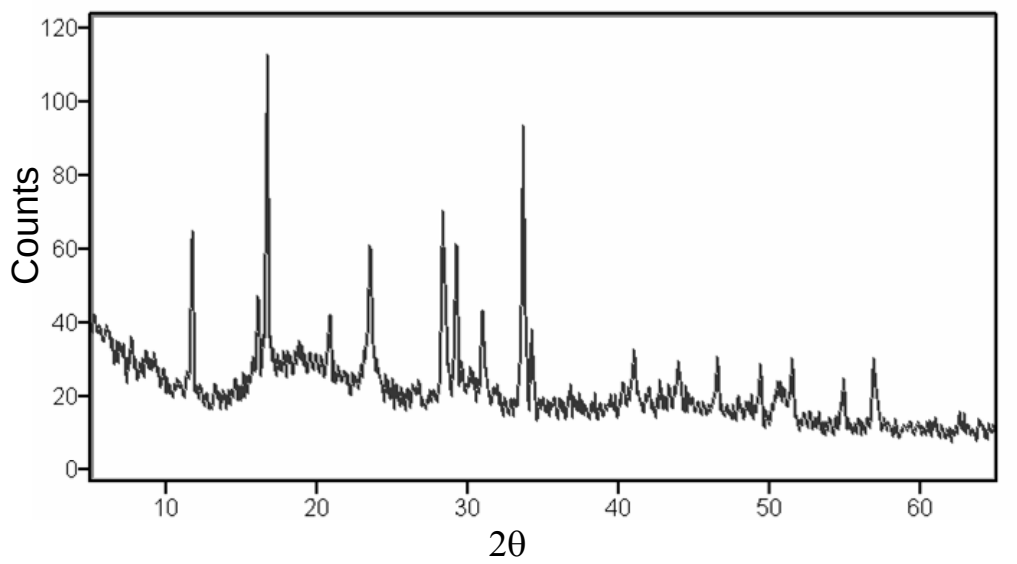

Figure 1. Observed XRD pattern for sulfite-rich but air-dried scrubber material.

TASKS 3, 4, and 7. Drying and Thermal Behavior:

Figure 2 reproduces the weight loss from wet sulfite-rich scrubber material at ambient atmosphere and temperature. As can be seen, the bulk of weight loss occurred during the first 24 hours, and thereafter the rate of weight loss decreased dramatically. It appears that for the development of composites from sulfite-rich scrubber material, the air-drying of the scrubber material for 48 hours will be adequate to sufficiently reduce the moisture content.

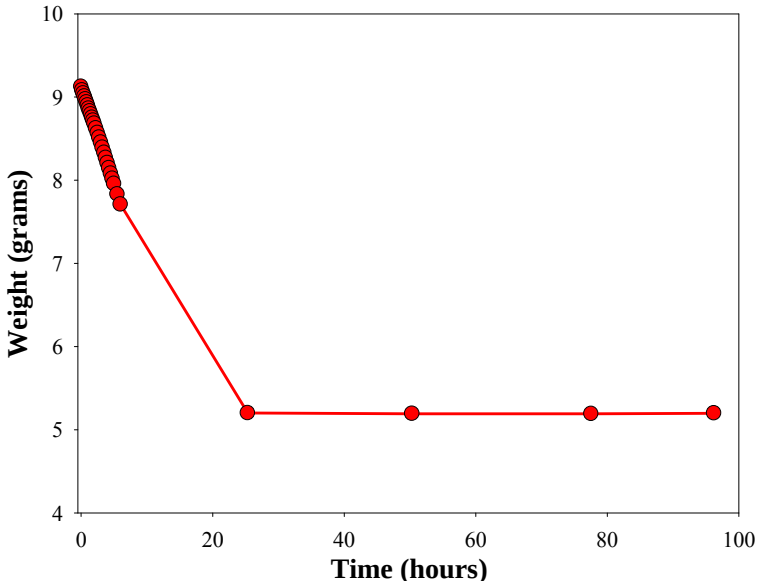

Figure 2. The weight loss from the sulfite-rich scrubber material at ambient temperature and atmosphere.

Figures 3 shows the effects of air drying time on the DSC curves obtained from sulfite-rich scrubber material. Strong endothermic reactions were observed at 134°C and 447°C. On air-drying the scrubber material at ambient temperature, the intensity of the 134°C endothermic peak steadily decreased and eventually disappeared for the sample which was air dried for 288 hours. The peak at 447°C persisted irrespective of the length of air-drying. The first endothermic peak at around 134°C represents the breakup and evaporation of loosely hydrogen-bonded water. The peak at 447°C indicated that the water associated with $CaSO_3$ in the scrubber material was much more strongly bonded.

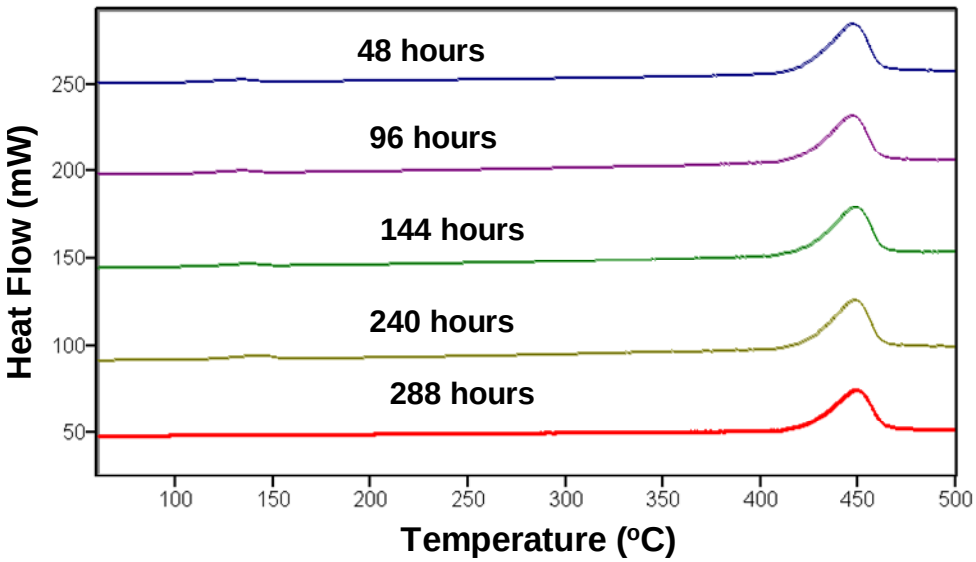

Figure 3. The DSC curves obtained from sulfite-rich scrubber material from Power Plant A air-dried at ambient temperature for different lengths of time.

Figure 4 reproduces the mercury concentration in the PPA and PPB scrubber materials as a function of air-drying time. Initially, the mercury concentrations in the PPA and PPB scrubber materials were 161 and 226 μg/kg, respectively. After one day of air drying, the mercury concentrations dramatically increased for both scrubber materials. This increase in concentration seems reasonable if it is argued that mercury in the scrubber material is not associated with water and as water evaporated the mercury concentration by weight increased. After 14 days of air drying time, the mercury in the PPA scrubber material increased to 283 μg/kg, while this increase was to 435 μg/kg for PPB scrubber material. The data presented in Figure 4 suggested that water continues to evaporate from the scrubber materials even after 14 days of air drying. However, it does seem more water was lost from PPB than PPA scrubber material for the first 14 days of air drying.

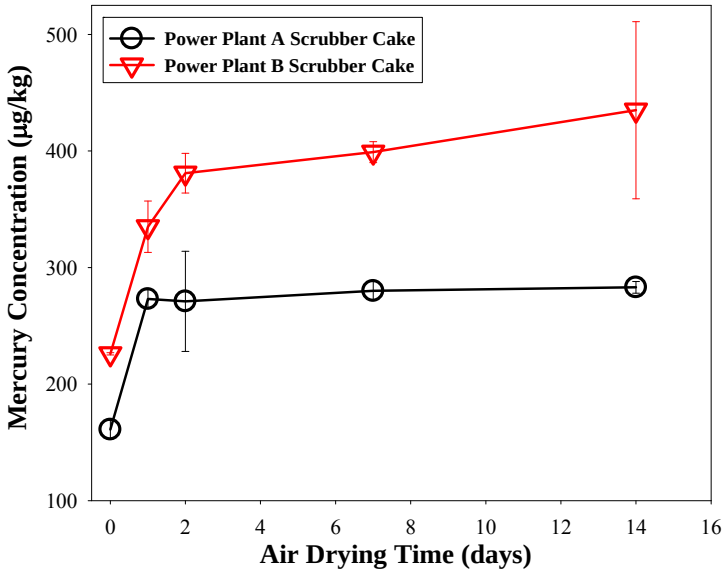

Figure 4. The effect of air-drying time on the mercury concentration in the scrubber materials.

As mentioned earlier, the development of value-added composites will require processing the scrubber material at $140^{o}C < T < 250^{o}C$ under high pressures ($1 MPa < P < 20 MPa$). When sulfite-rich scrubber material was subjected to heat treatment at $25^{o}C \leq T \leq 250^{o}C$ at ambient pressure under air, the mercury concentration in the scrubber material rapidly decreased as the temperature increased beyond $150^{o}C$. This can be clearly seen in Fig. 5. In fact, between $150^{o}C$ and $250^{o}C$, 35% of the mercury content of the scrubber material was lost, suggesting re-emission of mercury. This raised a serious concern whether during our product manufacturing significant amounts of mercury would be re-emitted. However, at higher pressures the thermodynamic properties of the solid mercury compounds are expected to be modified. Unfortunately, no detailed information is available in the literature listing how mercury compounds' vapor pressures are modified at elevated pressures. Moreover, at present the speciation of solid mercury compounds in the scrubber materials is lacking. Therefore, we subjected scrubber materials, obtained from PPA and PPB, to conditions, i.e., pressure and temperature, under which our composites will be formulated to ascertain whether our manufacturing approach will

require mercury scrubbing.

Figure 5 depicts how the fabrication temperature affected the mercury concentration in the scrubber materials. It appeared that the mercury behavior in the scrubber material for PPA was considerably modified at a higher pressure of 5.6 MPa. We did not observe any statistically significant loss of mercury from the PPA's scrubber material as long as the T $\leq 210^{o}$C. The PPA samples hot-pressed at 250^{o}C showed some loss of mercury from the scrubber material which was statistically significant. On the other hand, the scrubber material from PPB when hot-pressed at 250^{o}C did not show any statistically significant mercury loss.

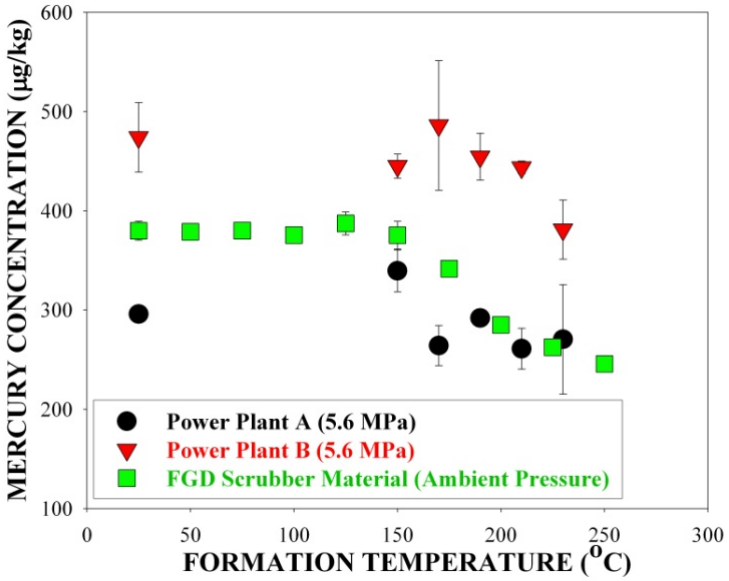

Figure 5. The effect of fabrication temperature on the Hg concentration of the scrubber materials from Power Plants A and B at 5.6 MPa.

Figure 6 shows how the formation pressure affected the mercury concentration in the scrubber material on hot-pressing it at 210^{o}C. When the scrubber material was heated under ambient pressure to 210^{o}C, we observed that sulfite-rich scrubber material lost about 32% of the mercury. As can be seen from Fig. 6, the higher pressures inhibited any statistically significant loss of mercury from scrubber material from PPA even though samples were hot-pressed at 210^{o}C. Unlike PPA scrubber material, we did observe a much larger variation in the mercury concentration of the PPB's scrubber material as a function of pressure. It appears at the lower pressures, i.e., P < 4 MPa, some mercury was volatized from PPB's scrubber material. However, as the pressure increased, no statistically significant loss of mercury was observed.

Task 2. Structural Analysis:

Figures 7 and 8 show the SEM photomicrograph of as-received scrubber material from PPA and PPB, respectively. The as-received scrubber materials, which were in wet cake form, were first air-dried at 25^{o}C for seven days prior to recording their photomicrographs. According to Randolph et al. [2], a wide variety of crystal growth

habits of calcium sulfite is observed depending upon dopants' and/or additives present in the liquor from which crystallites are precipitated. They suggested that in the absence of additives, typically platelet-like growth is the predominant crystal growth behavior. As can be seen from Figs. 7 and 8, both scrubber materials showed platelet-like structures.

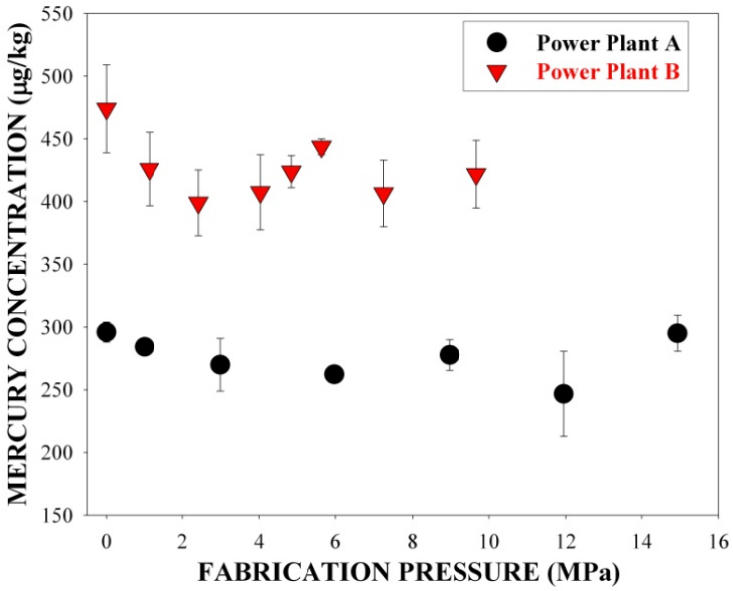

Figure 6. The effect of fabrication pressure on the Hg concentration of the scrubber materials from Power Plants A and B at 210°C.

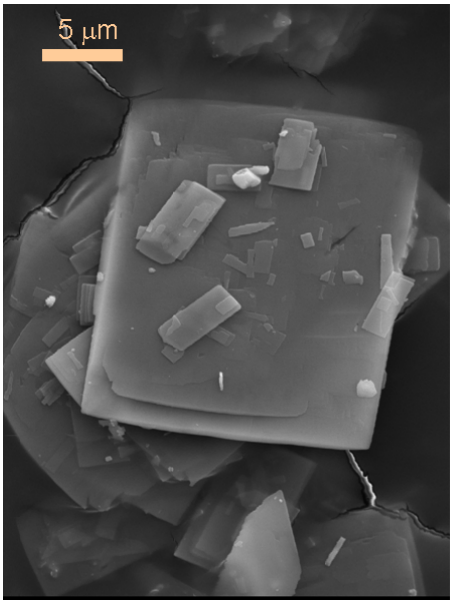

Figure 7: Scanning electron microscopy (SEM) picture of the as-received, but air-dried, sulfite-rich scrubber material obtained from Power Plant A.

However, while we observed a strong tendency for the crystallites from sulfite-rich material from Power Plant A to stack one above the other, no such tendency was observed for the scrubber material from Power Plant B. At present, it is not clear how

these different agglomeration behaviors would affect the fabrication of the composite materials from these two scrubber products. Another important observation was that while we did see some small fly ash particles in the scrubber material obtained from Power Plant B, we did not see similar fly ash particles in Power Plant A's scrubber material.

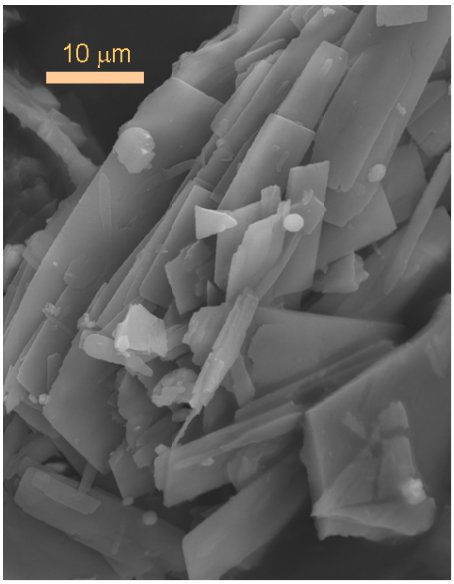

Figure 8: Scanning electron microscopy (SEM) picture of the as-received, but air-dried, sulfite-rich scrubber material obtained from Power Plant B.

TASKS 3 and 4. Thermal Behavior of Sulfite-Rich Scrubber Materials:

The thermal behavior of the as-received but air-dried scrubber material from Power Point A is shown in Fig. 9. The DTA curve showed six endothermic events at 109°C (broad peak), 161°C, 396°C (shoulder), 419°C, 722°C, and 1028°C and an exothermic event at 688°C. To facilitate the DTA analysis, we also recorded the thermal behavior of analytical grade $CaSO_3.nH_2O$ (Aldrich Chemical) under identical conditions used for scrubber materials. The $CaSO_3.nH_2O$'s DTA curve showed endothermic peaks at 115°C (broad peak), 160°C, 400°C, and 983°C, and a weak exothermic peak at 700°C. The broad endothermic peak observed at T < 120°C, for both scrubber material and $CaSO_3.nH_2O$, could be associated with the evaporation of the bulk-type water from the samples. The second endothermic peak at 161°C suggested the presence of more strongly bonded, perhaps hydrogen bonded, water in both samples. Gadalla and Gupta [1] and Zaremba et al. [3] have reported the thermal behavior of FGD scrubber materials, including DTA measurements. They suggested that the second endothermic peak at T < 200°C may be due to the presence of gypsum in the scrubber material. We discount this possibility for our scrubber material sample from Power Plant A because of the following:

(a) It is highly unlikely that the analytical grade $CaSO_3.nH_2O$ will have a significant amount of $CaSO_4.2H_2O$ to produce a strong but sharp peak in our DTA curves (see Fig. 9).

(b) The dehydration of gypsum occurs in two distinct steps, resulting in two sharp endothermic peaks at 125°C < T < 190°C. We did not observe these double peaks for our samples.

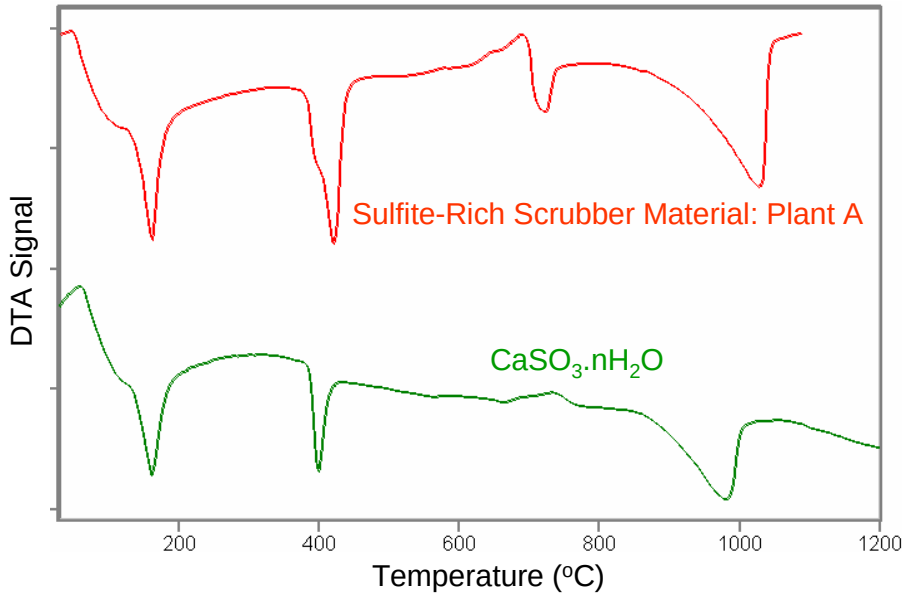

Figure 9. Differential thermal analyzer (DTA) curves of sulfite-rich scrubber material from Power Plant A (top curve) and of analytical grade hydrated calcium sulfite (bottom curve). The DTA curves were recorded under N_2 gas environment.

(c) Gypsum undergoes a structural phase transition at ~ 360°C, which results in an exothermic peak. We did not observe this exothermic peak for our samples though we did see this peak when gypsum samples were investigated.

The endothermic peak observed at 400°C for $CaSO_3.nH_2O$ could be associated with the following decomposition reaction [1,3],

$$(CaSO_3)_x(CaSO_4)_{1-x}\cdot 0.5H_2O\ (s) \rightarrow (CaSO_3)_x(CaSO_4)_{1-x}\ (s) + 0.5H_2O\ (\uparrow) \quad \text{eq.(1).}$$

The fact that we observed two endothermic peaks at 396°C and 419°C for scrubber material from Power Plant A raises the possibility of a more complex structure for the calcium sulfite crystallites produced during the scrubbing process.

The weak exothermic peak at 670°C < T < 705°C suggested the disproportionation reaction of $CaSO_3$ [3,5], i.e.,

$$4CaSO_3(s) \rightarrow 3CaSO_4(s) + CaS \qquad \text{eq.(2).}$$

We observed an endothermic peak at 722°C for the scrubber material from Power Plant A but not for analytical $CaSO_3.nH_2O$. Zaremba et al. [3] have attributed this endothermic reaction to the decomposition of $CaCO_3$, i.e.,

$$CaCO_3(s) \rightarrow CaO(s) + CO_2(\uparrow) \qquad \text{eq. (3).}$$

Because Power Plant A uses limestone as a scrubbing material, therefore, it is not surprising to see the presence of $CaCO_3$ in our samples. It is also consistent with the fact

that we should not have observed this exothermic reaction for analytical $CaSO_3.nH_2O$, which is the case here.

The final endothermic peak observed for both scrubber material from Power Plant A and $CaSO_3.nH_2O$ at $950^oC < T < 1050^oC$ could be assigned to the following reactions [1,3]:

$$CaS(s) \rightarrow CaS_x(s) + (1\text{-}x)S(\uparrow) \qquad \text{eq. (4)},$$

and

$$CaSO_3(s) \rightarrow CaO(s) + SO_2(\uparrow) \qquad \text{eq. (5)}.$$

The mass loss of scrubber material from Power Plant B is shown in Fig. 10, while Fig. 11 depicts the DTA curve obtained at $50^oC < T < 1250^oC$ under nitrogen gas environment. Tables 2 and 3 summarize the thermal events observed for Power Plant B's scrubber material. The fact that 6 weight percent loss could be associated with the decomposition of $CaCO_3$, indicated that a significant amount of $CaCO_3$ is present in the scrubber material from Power Plant B. The observed DSC curve under O_2 gas environment is shown in Fig. 12, and the observed thermal events' parameters are listed in Table 4. The DSC curve showed two endothermic peaks at $T < 210^oC$ suggesting that under an oxygen-rich environment water would be lost from the scrubber material in two distinct steps.

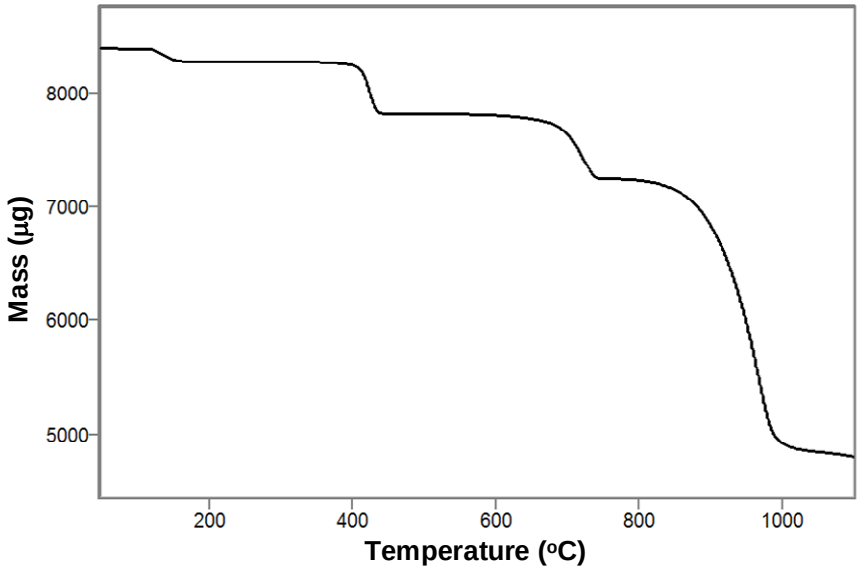

Figure 10. Thermal gravimetric (TGA) curve of sulfite-rich scrubber material obtained from Power Plant B. The TGA data were recorded under N_2 gas environment.

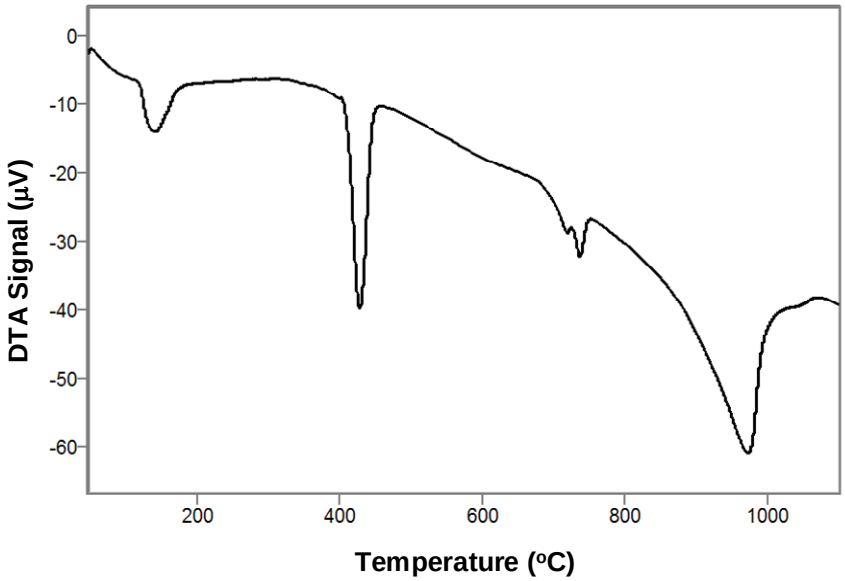

Figure 11. Differential thermal analyzer (DTA) curve of sulfite-rich scrubber material from Power Plant B. The DTA curve was recorded under N_2 gas environment.

Table 2. The thermal events observed for sulfite-rich scrubber material obtained from Power Plant B as recorded by TGA method.

Thermal Event Number	Mass Loss Begins (°C)	Mass Loss Ends (°C)	Peak Mass Loss Temperature (°C)	Weight Loss (%)	Assignment
1	121	151	136	1.3	H_2O evaporation
2	410	432	421	5.2	Eq. 1
3	692	736	714	6.2	Eqs. 2 and 3
4	909	987	947	27.4	Eqs. 4 and 5

Table 3. The DTA results for scrubber material from Power Plant B.

Peak Number	Peak Temperature (°C)	Peak Area (µV.s/mg)	Assignment
1	139	90	H_2O evaporation
2	427	213	Eq. 1
3	719 and 736	67	Eq. 3
4	970	712	Eq. 4 and 5

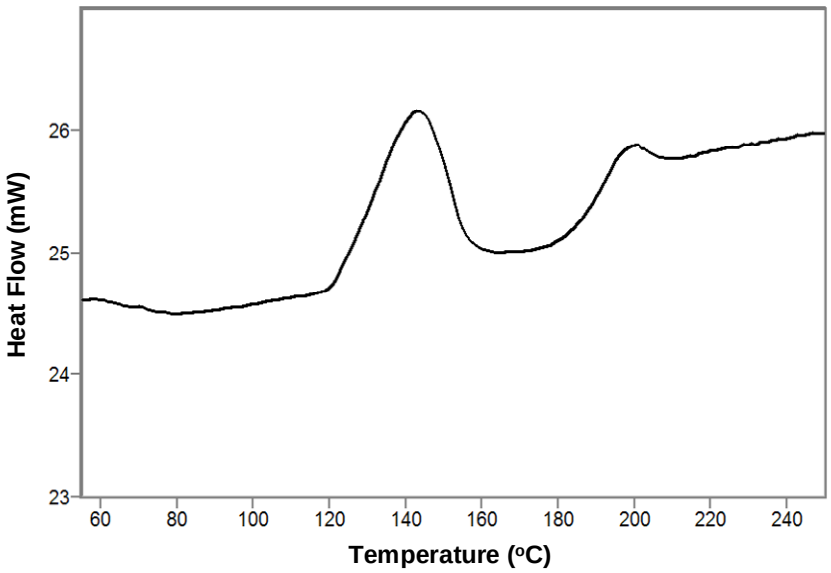

Figure 12. Differential scanning calorimetric (DSC) curve of sulfite-rich scrubber material from Power Plant B. The DSC curve was recorded under O_2 gas environment.

Table 4. This table summarizes the thermal parameters associated with the two endothermic events observed for Power Plant B's scrubber material. The data were obtained using the DSC technique under oxygen gas environment.

Peak Number	Peak onset (^oC)	Peak Temperature (^oC)	Delta H (J/g)
1	123	143	23.4
2	189	199	5.4

Task 7. Effect of Composite Formulation Conditions on the Structure of Scrubber Materials:

The fabrication of wood-substitute composites from sulfite-rich scrubber materials would require subjecting these materials to high temperature and high pressure. Therefore, it was important that we understood how the chemical and crystalline structures of the scrubber materials were affected when subjected to high-pressure at high-temperature.

Pressure Effect: To evaluate the pressure effects on the structure of scrubber materials at high-temperature, we subjected the scrubber material to a load ranging from 500 lbs to 7500 lbs. The loads were applied at 210^{o}C. The air-dried scrubber material was mixed with a known amount of water, and the resulting paste was poured into a 2-inch diameter hardened stainless steel die. The die was inserted between the platens of a floor mounted high-temperature, high-pressure press. The plunger which fitted into the die applied the load to the sample. The platens were pre-heated to 210^{o}C before the die was introduced into the press. The sample was held at the desired load for 1 hour before the pressure on the die was released and the die removed from the platens. The resultant disk was ejected from the die, and the sample was subjected to various analyses.

Figures 13 and 14 show how a load of 500 lbs (P = 160 psi or 1.10 MPa) and 7500 lbs (P

= 2390 psi or 16.5 MPa), respectively, affected the crystallites of the scrubber material from Power Plant A. It can be seen from Fig. 13 that for a pressure of 160 psi, most of the crystallites maintained their platelet-like shape at 210°C. However, much more fines (< 2 μm) were observed relative to as-received scrubber material suggesting that fines were generated during the application of the load. Increasing the applied pressure to 2390 psi substantially increased the generation of fines as can be seen from Fig. 14. There was also evidence that an applied load of 7500 lbs compresses the crystallites indicating that scrubber material is a soft material and will compress under our product manufacturing conditions.

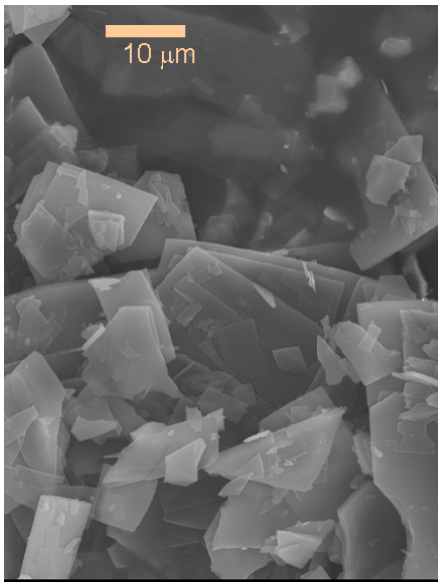

Figure 13. SEM picture showing how hot-pressing the scrubber material at 210°C under a load of 500 lbs affected the structure of sulfite-rich sludge from Power Plant A.

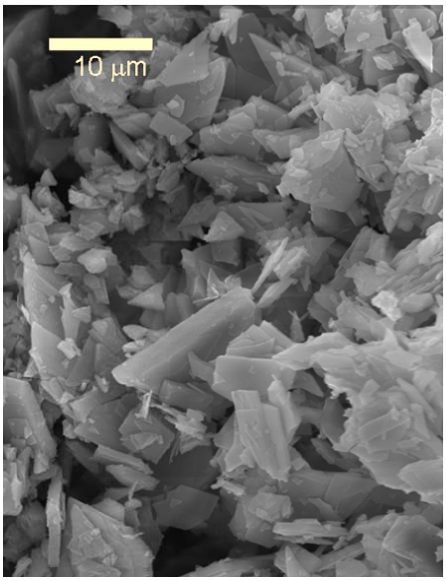

Figure 14. SEM picture showing how hot-pressing the scrubber material at 210°C under a load of 7500 lbs affected the structure of sulfite-rich sludge from Power Plant A.

Figure 15 reproduces how the applied load affected the FTIR spectra of scrubber material from Power Plant A. Because we recorded our FTIR spectra using smears of mineral oil, it was not possible to monitor the quantitative changes in the intensities of the observed oscillators. However, to monitor how the applied pressure at 210°C affected the structure of the scrubber material we generated the intensity ratios. The ratios were generated by dividing the S-O bending mode vibration intensity. Figure 16 shows how the applied load affected the vibrational intensities' ratios of the scrubber material. As can be seen

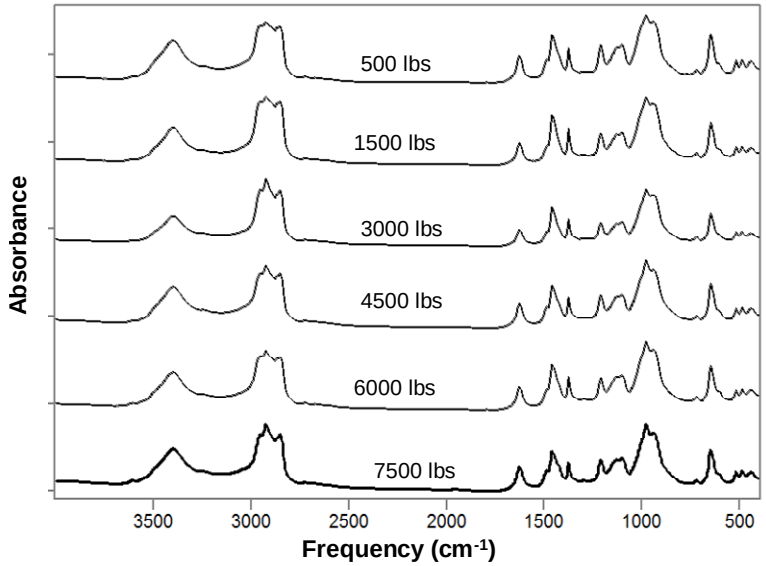

Figure 15. Fourier transform infrared (FTIR) spectra of sulfite-rich scrubber material depicting how the applied load affected the structure of the scrubber material from Power Plant A.

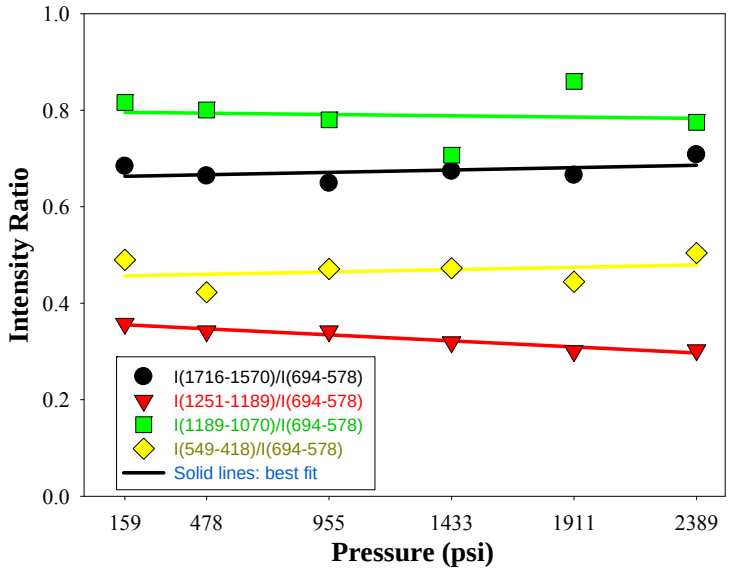

Figure 16. This figure shows how the hot-pressing pressure at 210°C affected the intensity ratios of the observed infrared vibrational bands of the sulfite-rich scrubber material from Power Plant A.

from this figure, there was no discontinuity in the graph which would have suggested a change in the structure of the calcium sulfite. Therefore, we conclude that the structure of the scrubber material remains intact under the applied load.

Temperature Effect: How the composite fabrication temperature would affect the structure of scrubber material under high-pressure was evaluated by subjecting the scrubber material to temperatures in the range of 150°C to 230°C under load of 3500 lbs (P = 1115 psi or 7.7 MPa). The temperature treatments were carried out in a stainless steel die as described earlier. Figures 17 and 18 show how the applied temperature of 150°C and 210°C, respectively, affected the crystallites of the scrubber material from Power Plant A. It appears from these photomicrographs that the hannebachite crystallites were compressed and showed considerable amounts of fine generation at 210°C. It is possible that during composite fabrication the compression of the crystallites and the generation of fines could contribute to higher densities of the final product.

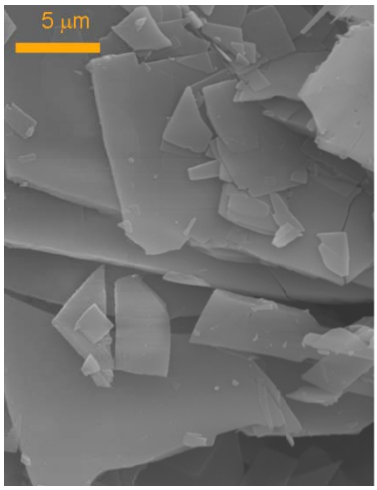

Figure 17: SEM picture showing how hot-pressing the scrubber material at 150°C under a load of 3500 lbs affected the structure of sulfite-rich sludge from Power Plant A.

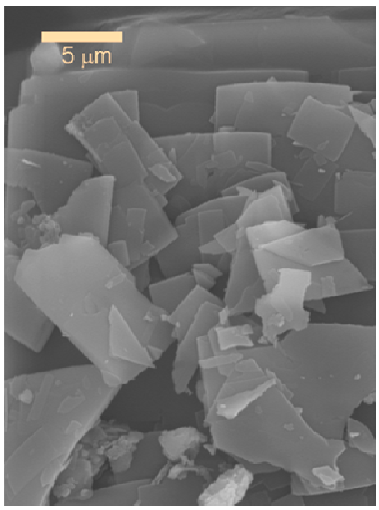

Figure 18. SEM picture showing how hot-pressing the scrubber material at 210°C under a load of 3500 lbs affected the structure of sulfite-rich sludge from Power Plant A.

Figure 19 shows how the hot-pressing temperature affected the vibrational spectra of sulfite-rich scrubber material from Power Plant A. Our thermal analysis results, described earlier, suggested that at ambient pressure bulk water as well as some weakly hydrogen-bonded water were lost when the scrubber material's temperature was raised to 200°C. It should be noted from Fig. 20 that the intensity of the water oscillators, in the stretching (3700 – 2900 cm^{-1}) and bending (1800 – 1550 cm^{-1}) region, was not affected as a function of hot-pressing temperature. This was surprising. It appeared that a pressure of 1115 psi on the sample inhibited water loss. Figure 20 reproduces how the hot-pressing temperature affected the structure of the scrubber material. Again, no discontinuity in the intensity ratios was observed as a function of temperature. Therefore, it was reasonable for us to conclude that under our composite fabrication temperature the sulfite-rich scrubber material will maintain its structure.

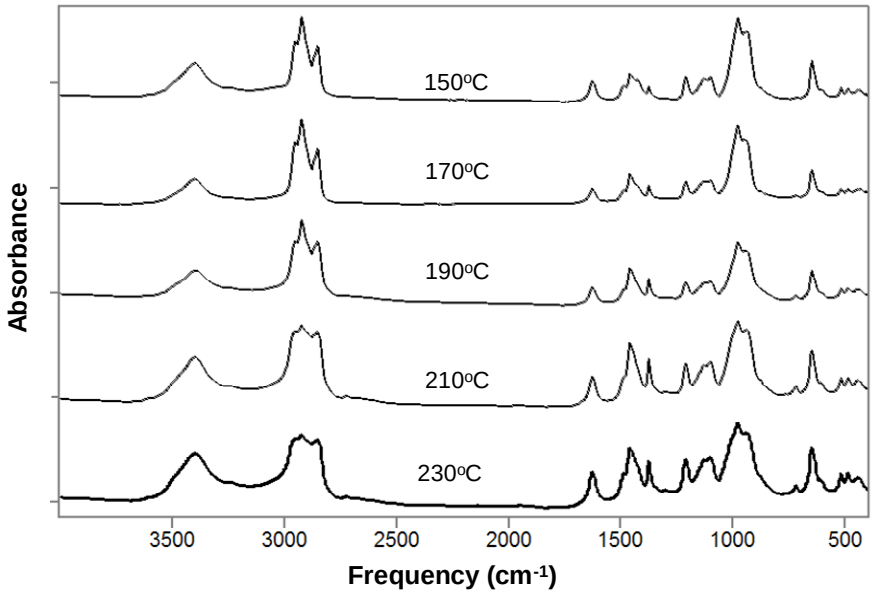

Figure 19. Fourier transform infrared (FTIR) spectra of sulfite-rich scrubber material depicting how the formation temperature affected the structure of the scrubber material from Power Plant A when hot-pressed under a load of 3500 lbs.

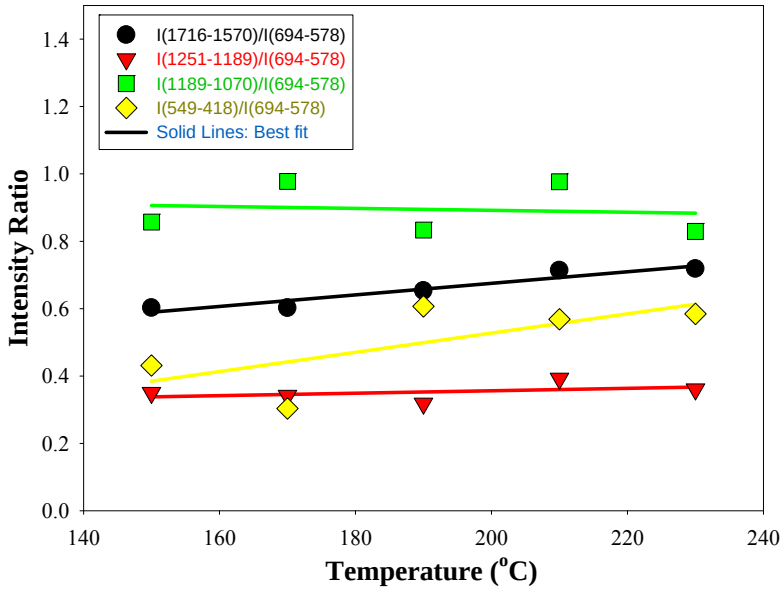

Figure 20. This figure shows how the hot-pressing temperature at a pressure of 3500 lbs affected the intensity ratios of the observed infrared vibrational bands of the sulfite-rich scrubber material from Power Plant A.

Tasks 5 through 8. Development and Performance of Wood-Substitute Composites:

Typical composite materials have two or more distinct phases, usually referred to as a matrix and fillers, additives, or reinforcements. Sulfite-rich scrubber material could be formed into a solid sample just by the addition of water, which results in the reaction where weak hydrogen bonds are formed that hold the sample together. The material, however, was very brittle and dense. To achieve a high strength and modulus, which was comparable in magnitude to the load bearing wood material, we proposed to develop composite materials from sulfite-rich scrubber material and matrix of natural fibers and polymers. Having a matrix composed of such natural polymers as cellulose, hemicelluloses, and lignin, which are the same polymers that make up the chemical composition of wood, would give our composite material derived from scrubber sludge wood-like appearance and behavior. Moreover, it was expected that our crop matrix material would help in reducing the density of the final product.

Crop A material used in this study could be formed into a composite material all by itself by applying specific temperature and pressure. Figure 21 shows a composite material formed mainly from the Crop A matrix, reinforced with 10% of scrubber material from PPA. This composite was formed at 190^{o}C under a load of 83 MPa. It can be seen from the figure that the natural fibers have fused together to form a composite structure.

Figure 22 depicts the mechanical behavior, i.e., stress-strain curve, of the composite derived with 10% scrubber material. It can be observed that the composite has fairly high flexural strength and high modulus. Typically, composites derived with 10% scrubber material were stiff and broke at the strain values which were lower than 1%. However, it should be noticed that these composites did not undergo catastrophic brittle failure. It appears that the fibers held the composite together even after cracks had been generated

by the applied load.

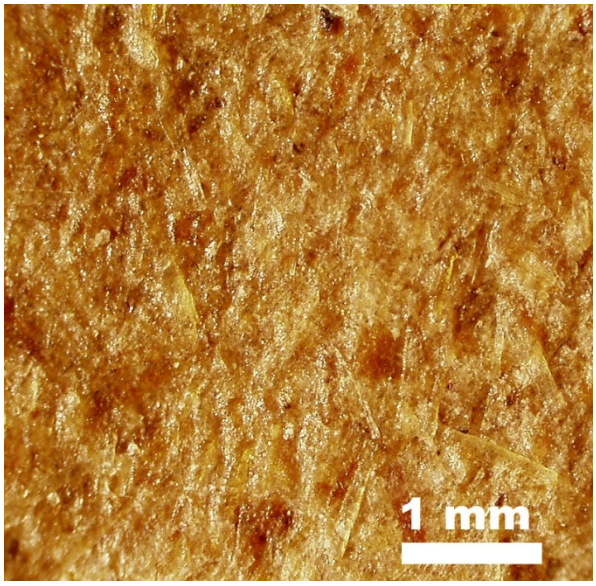

Figure 21. This picture shows the natural fiber matrix composite formed with 10 wt% sulfite-rich scrubber material.

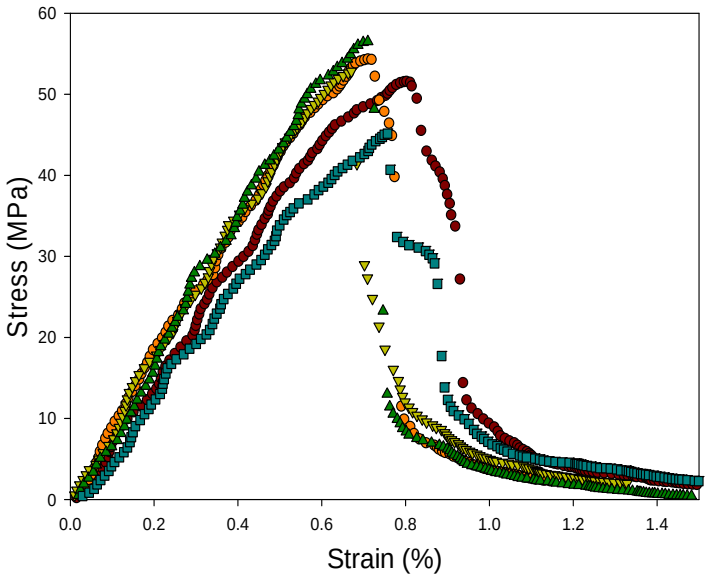

Figure 22. Stress-strain behavior of natural fiber matrix-based composite derived with scrubber material.

Specific properties of matrix material and eventually of the composites depend significantly on the additives used. Our matrix mainly utilizes natural resins to hold the composite together, however, high pressures and high temperatures are required to access these polymers which may not always be a viable processing route. Therefore we have examined how small amounts of various natural and synthetic polymeric materials may enhance the properties of our composites and possibly reduce the fabrication costs.

Both sulfite rich scrubber material and Crop A material are in the fine powder form, which poses a challenge when trying to add a small quantity of liquid-based resin into the mixture. The resin gets adsorbed by the powder which inhibits good dispersion. One of the ways to get around this problem could be by using a water-based polymer and mixing a polymer in a water-sludge-fiber slurry in order to achieve uniform dispersion. Figure 23 represents flexural strength and density results of such an attempt, where 50/50 scrubber-crop mixture was combined with a water-dispersible commercial epoxy resin.

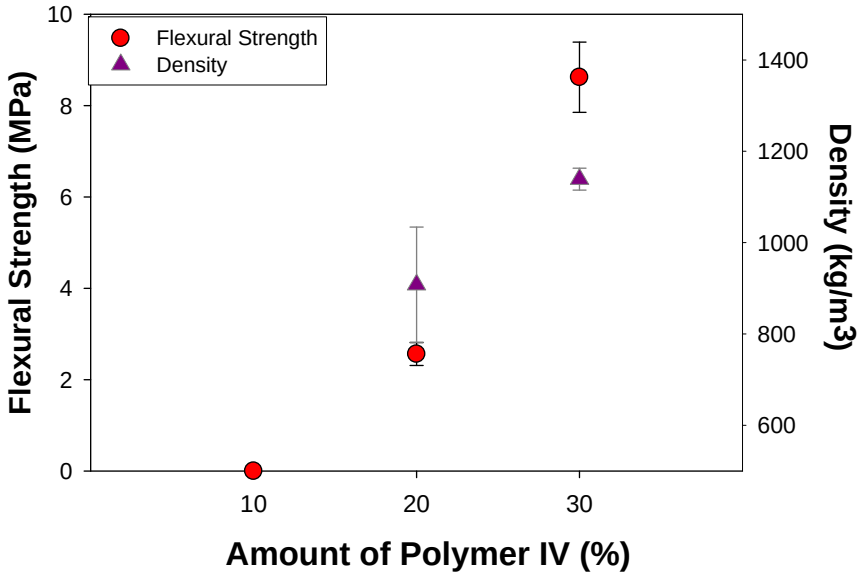

Figure 23. Strength and density of the sample as a function of amount of water soluble commercial polymer.

Although good dispersion of the fibers and additives was observed in the composites, the composite materials suffered from low flexural strength. The density of the composites was low though (see Fig. 23). It should be noticed that even the composites, which contained 30% resin by weight, barely reached the strength of 9 MPa (1305 psi). It was felt that the amount of water used to formulate these composites may have contributed significantly to the observed reduced flexural strength. Therefore, we varied the water concentration used to formulate the composites from water-soluble polymer IV. How the water content affected the mechanical properties is shown in Fig. 24, while typical stress-strain behavior of the composites is depicted in Fig. 25. It is evident from the graph that the amount of water in the initial mix did play an important role in determining the mechanical properties of the formulated composites. The composites formulated with 20 g water yielded the highest mechanical strength for this series. A composite containing 10 g of water showed poor performance mainly due to the inadequate dispersion of the additives. This was because the mixture was very thick and difficult to mix. The sample containing 30 g of water was too soft to be even tested. One of the reasons for such a low flexural strength of these samples is low fabrication temperature of the composites, which was limited due to the specifications of the polymer used. Fabrication temperature of 120^{o}C was used, which was the curing temperature of the water-based resin. However, by using such a low temperature, we could not observe the benefits of the natural resins, the condensation of which require much higher processing temperatures. On the other hand,

the water soluble polymers allowed us to fabricate composites at the very low pressure of 1.2 MPa (174 psi). Moreover, the composites resulted in low densities ranging between 900 kg/m^3 and 1300 kg/m^3. The stress-strain results of these composites also exhibited the desired behavior. Figure 25 depicts stress vs. strain curves. As can be seen from this figure, though composites underwent failure at around 1% strain they did not show classical brittle behavior.

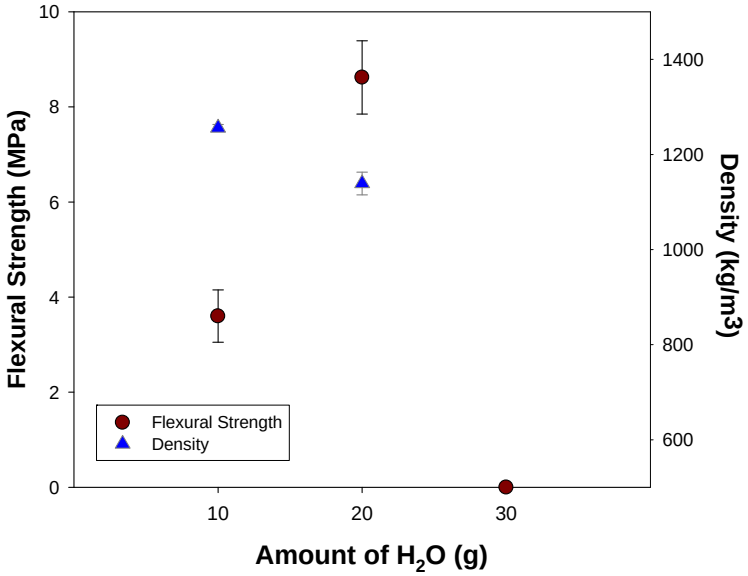

Figure 24. Strength and density dependence on the amount of water used for the composite fabrication from natural matrix, scrubber material, and water soluble polymer IV. Total mass of other ingredients was 25 g.

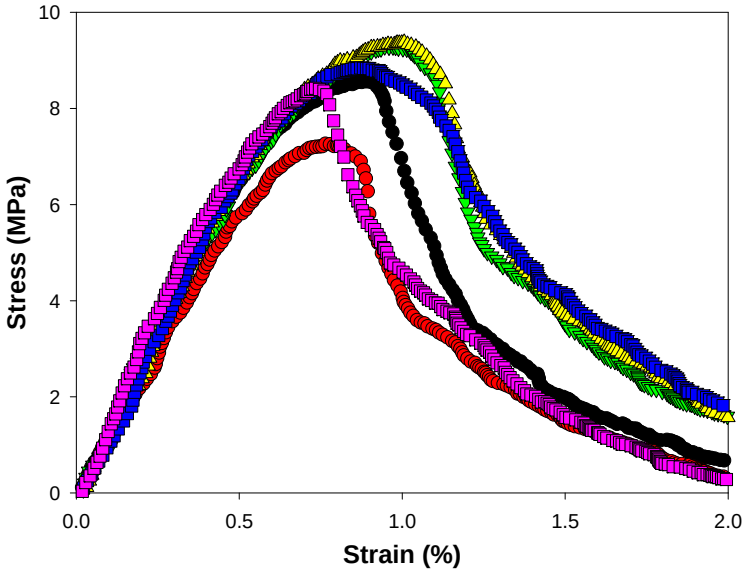

Figure 25. Stress vs. strain behavior of composite material derived from water soluble polymer IV.

THIS PAGE CONTAINS PROPRIETARY INFORMATION

THIS PAGE CONTAINS PROPRIETARY INFORMATION

THIS PAGE CONTAINS PROPRIETARY INFORMATION

THIS PAGE CONTAINS PROPRIETARY INFORMATION

THIS PAGE CONTAINS PROPRIETARY INFORMATION

THIS PAGE CONTAINS PROPRIETARY INFORMATION

THIS PAGE CONTAINS PROPRIETARY INFORMATION

Figure 35 shows the mechanical properties of commercial WPC fabricated from thermoplastic HDPE. The density of the product ranged from ~1025 kg/m^3 to ~1250 kg/m^3, while the strength varied between ~ 10 MPa (1450 psi) to ~ 18 MPa (2610 psi). Similar to the strength, flexural modulus of the WPC increases as the density of the product increases. It can be seen from Figs. 36 and 37 that the increase in the concentration of thermoplastic HDPE in the mix not only increases the strength of the material but also its density. Therefore, to successfully compete against the current WPC products on the market, the products developed from sulfite-rich scrubber material must not only be cheaper but must also have superior mechanical properties.

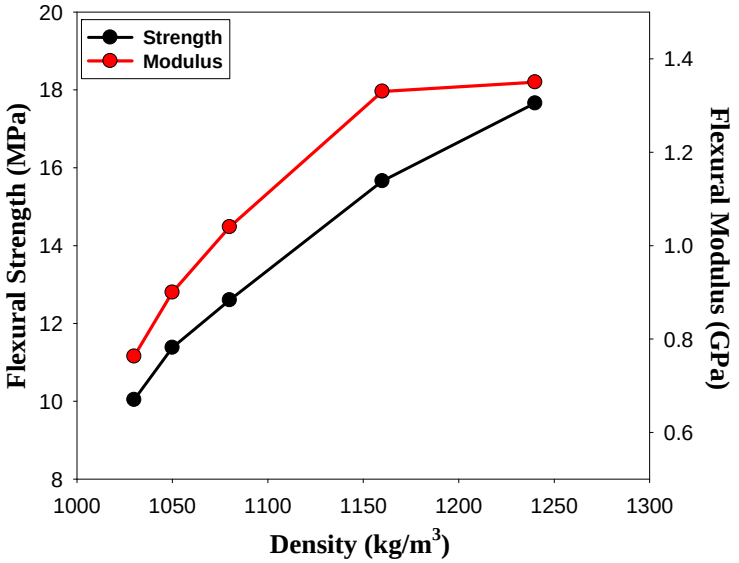

Figure 35. The mechanical properties of commercial wood plastic composites.

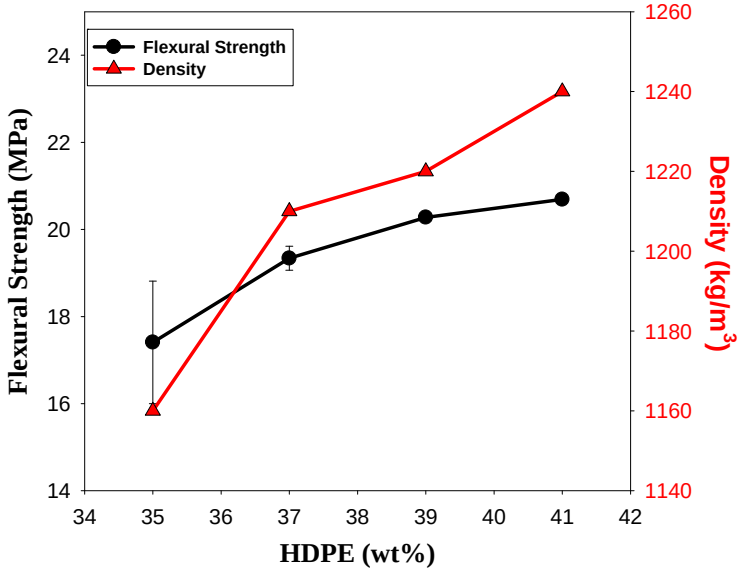

Figure 36. How the thermoplastic HDPE concentration affected the mechanical properties of wood plastic composites.

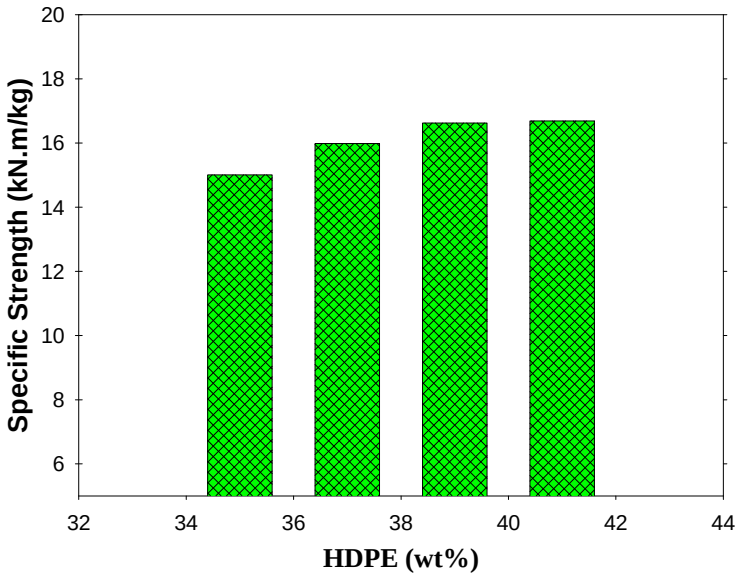

Figure 37. How the thermoplastic HDPE concentration affected the specific strength (= (flexural strength)/density) of wood plastic composites.

We formulated our WPC materials from sulfite-rich scrubber material, natural fibers and HDPE. To keep the cost of our products low, we used recycled HDPE. Recycled HDPE was generated from post-consumer milk containers. The plastic bottles were initially shredded, using a cutting mill fitted with a screen with 8 mm mesh size. Following that, the shreds were further reduced with the help of a cyclone grinding mill, which resulted in HDPE beads with the average size of about 100 μm in diameter.

HDPE – scrubber material – fiber composites were fabricated via compression molding. Raw materials were thoroughly mixed with a motorized high speed (propeller shaped) mixing rod and were molded in the 50 mm diameter high pressure stainless steel die. Two series of samples were prepared. First, HDPE to additive ratio was varied, while keeping scrubber material-to-natural fiber ratio fixed 4:1 (by weight). The second series contained fixed HDPE content (70% by weight), while scrubber material-to-natural fiber ratio was varied. Composites were cut into approximately 5 mm sections using a band saw for flexural strength test.

Figure 38 shows the flexural strength and density variation as the amount of additive (at 4:1 scrubber material-to-natural fiber ratio) changed. There was an initial drop in flexural strength observed as the filler was introduced into the composite. The strength values dropped to ~ 20 MPa, about half of that of the pure HDPE. The strength was, however, maintained as the filler concentration was increased up to 40 wt% after which it slowly declined. The density followed the opposite trend of the flexural strength as the additives were introduced into the polymer. This was expected because the sulfite-rich FGD material is denser than both HDPE and natural fibers. This was also reflected in Fig. 39, which shows how the flexural strength and density of the composites were affected when the HDPE concentration was kept fixed at 70 wt% but the FGD material-to-natural fibers ratio was varied. Figure 38 shows that calcium sulfite-to-miscanthus ratio of 1:1 might

yield the optimum performance with the flexural strength of 26 MPa and density values just around 1000 kg/m^3. The stress vs. strain behavior of this composite was compared to the stress vs. strain behavior of pure HDPE sample in Figure 39.

Other than the conservation of natural resources, there are two main reasons for incorporating both calcium sulfite and natural fibers into the HDPE matrix. Not only should substitute engineered wood composites have high enough strength but they should also mimic the appearance and workability of wood. Though recycled but pure HDPE sample by itself has a higher flexural strength, it is a very flexible and ductile material, which makes it more difficult to work with using conventional wood-working tools. For example, this type of material may be difficult to nail, or drive a screw into, as well as chisel, or even cut. From the stress vs. strain behavior of pure HDPE, shown in Fig. 39, it was evident that the material is very elastic and stretches up to 6% of strain without breaking. After the incorporation of sulfite crystallites and natural fibers, the stress vs. strain behavior more closely resembled that of natural wood. While material did fail at the higher strain values, the failure was gradual. It is also interesting to note that the stress values at 2% of strain for both of the samples were about the same around 22 MPa.

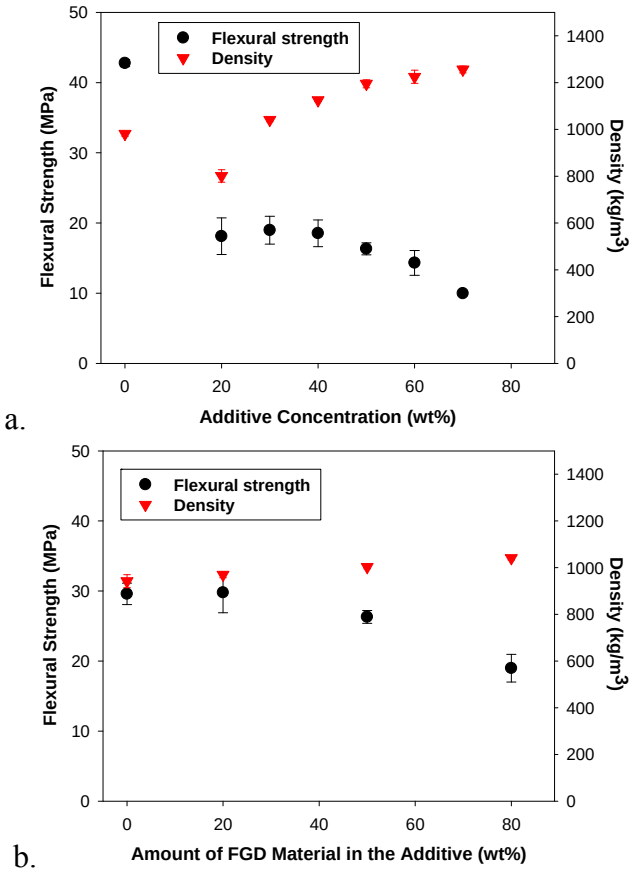

Figure 38. Flexural strength and density of HDPE composites: a) as a function of additive concentration at 4:1 scrubber material-to- fiber ratio, and b) as a function of the amount of scrubber material (HDPE was fixed at 70 wt%).

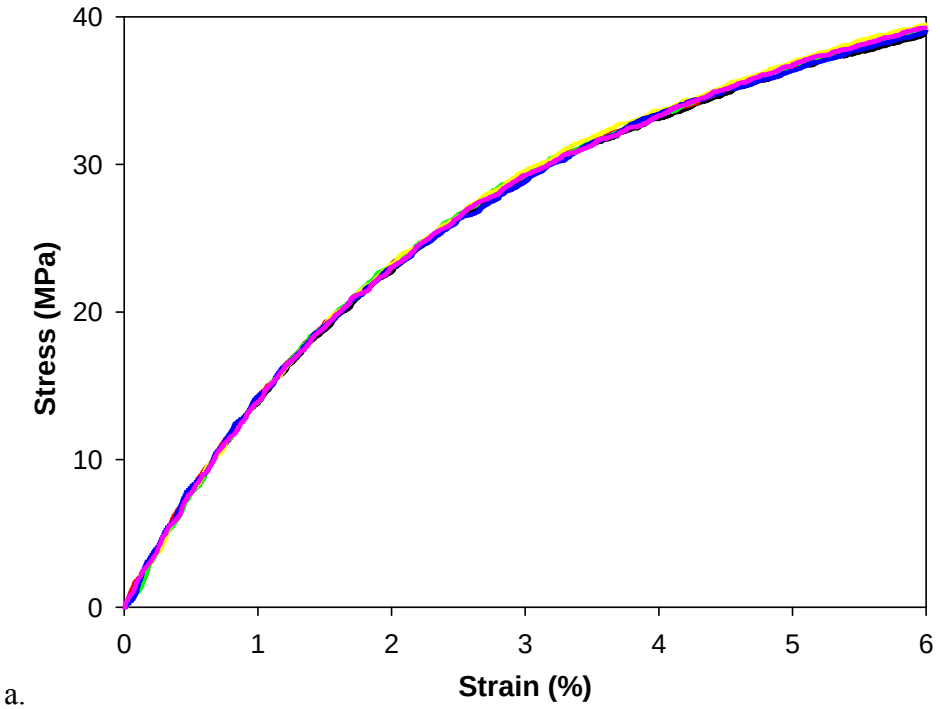

a.

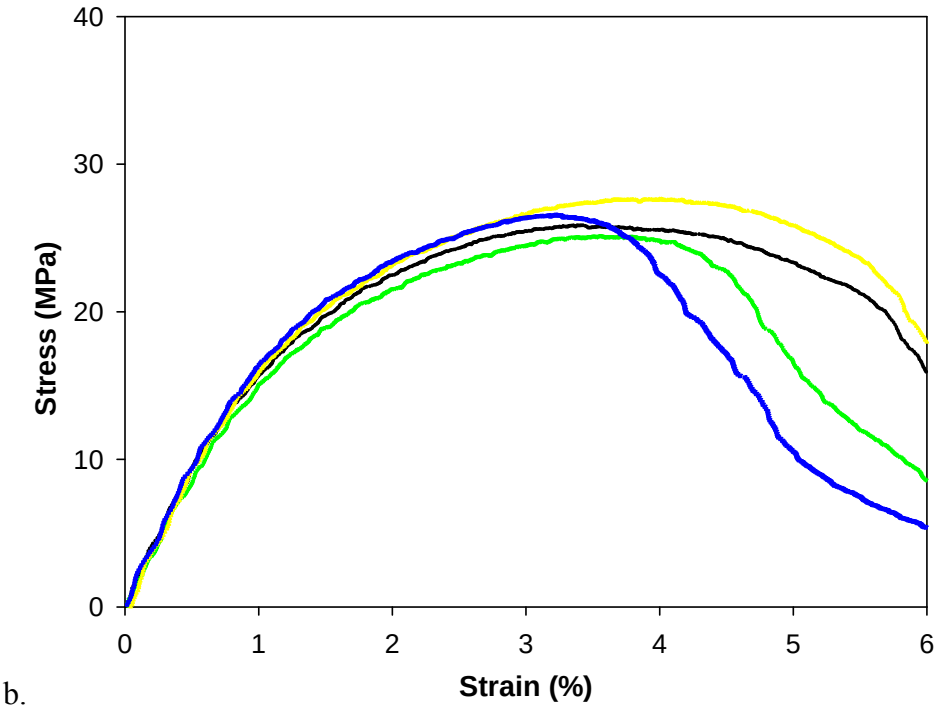

b.

Figure 39. Stress vs. strain characteristics of pure but recycled HDPE sample (a), and of composite material containing 70 wt% of HDPE, 15 wt% of scrubber material, and 15 wt% of natural fibers (b).

CONCLUSIONS AND RECOMMENDATIONS

In this cost-share project, we explored whether it was possible to develop wood-substitute products from FGD sulfite-rich scrubber material. To accomplish this, a range of characterization, mechanistic, and product development experiments was undertaken. The following summarizes the main findings of our project:

1. Gravimetric measurements suggested that water was rapidly lost at the ambient temperature from the scrubber cake for the first 24 hours, and thereafter there was a dramatic decrease in the rate of water evaporation. However, for our product manufacturing, 24 hours of scrubber cake drying would be adequate.
2. The physical structural analysis of the sulfite-rich scrubber material, obtained from two different power plants, indicated that the crystallites were typically hannebachite in appearance, i.e., platelet-like crystallites of $CaSO_3.0.5H_2O$. Our SEM measurements also revealed that the scrubber material from one of the power plants had a strong tendency to agglomerate in which crystallites stacked one over the other rather than forming spherical-looking agglomerates. The scrubber material from the second power plant did not show this behavior.
3. The XRD diffraction of the as-received, but air-dried, scrubber cake indicated peaks at 11.7, 16.1, and 16.7 degrees, thus, suggesting the scrubber cake to be a mixed phase of $CaSO_3.0.5H_2O$, $CaSO_3.4H_2O$, and $(CaSO_4)_x.(CaSO_3)_{1-x}.nH_2O$.
4. Our DSC measurements indicated that the products developed from the sulfite-rich scrubber materials would be stable as long as the temperature was $< 400^oC$.
5. Our results indicated that the mercury concentrations in sulfite-rich scrubber material should be determined at least after 14 days of air drying ($T < 30^oC$) time because of continued water loss from the scrubber material.
6. On subjecting the scrubber material to high temperatures and pressures typically expected during our product development, we did not observe any statistically significant emission of mercury from the scrubber cake.
7. The detailed thermal measurements, i.e., TGA and DTA analyses at $50^oC \leq T \leq 1250^oC$, on the scrubber materials suggested that there are four main thermal events by which scrubber material from both power plants decomposed. Consistent with the DSC results, TGA and DTA measurements also reinforced our suggestion that in our wood-substitute composites, the scrubber material would not decompose at $T < 400^oC$. Above 400^oC, half water molecule were lost from the hannebachite crystallites, thus this might retard the flammability of our composites.
8. The exposure of sulfite-rich scrubber material to high-pressure (ambient pressure $\leq P < 3000$ psi) and high-temperature ($25^oC < T < 250^oC$) resulted in the compression of hannebachite crystallites though they maintained their platelet-like shape. However, it was noticed that higher pressures, i.e., $P > 1100$ psi, and higher-temperatures, i.e., $T > 200^oC$, generated a considerable number of fines. The production of these fines during composite fabrication conditions could result in higher densities of the material. The vibrational (infrared) analysis of the scrubber materials, which were subjected to high-temperatures at high-pressure, indicated that the sulfite-rich scrubber materials retained their chemical structure under the above-mentioned conditions.

9. Our results showed that it was feasible to make composite materials from FGD sulfite-rich scrubber material with flexural strengths up to 90 MPa (13,050 psi). Formation pressure and temperature played an important role, besides the ingredients, in determining the final strength and elastic properties.
10. Depending upon the type of polymer, it appeared that wood-substitute composites could be formulated with sulfite-rich scrubber material with a concentration ranging from 60 wt% to 75 wt%. It also appears that the density of the composites derived from sulfite-rich scrubber material could be lowered either by the addition of fly ash or hollow spherical particles. However, hollow spherical particles were more effective in lowering the density yet maintaining the higher strength.
11. Our results suggest that post-curing the wood substitute composites developed from sulfite-rich scrubber material resulted in defect sites and micropores. This effectively reduced the density slightly though the strength of the composite also decreased by about 4 MPa. Therefore, it is recommended that wood-substitute composites fabricated from scrubber material not be subjected to post-curing.
12. We demonstrated that by combining recycled thermoplastics obtained from consumer recycled products with scrubber materials load-bearing wood plastic composites could be formulated. Flexural strengths in the range of 15 MPa – 30 MPa were achieved, which is comparable to other engineered-wood composites. Storage modulus at sub-ambient temperatures was improved with the addition of calcium sulfite into recycled thermoplastic.

REFERENCES

1. A. M. Gadalla and A. Gupta, Ind. Eng. Chem. Res. **33**, 1145, 1994.
2. A. D. Randolph, D. J. Kelly, and B. Keough, "Calcium Sulfite and Calcium Sulfate Crystallization. Volume 1.: Effect of Crystallizer Type on Gypsum Size Distribution", EPRI Report 1013-3, 1986.
3. T. Zaremba, A. Dukowicz, J. Hehlmann, W. Mokrosz, and E. Kujawska, J. Thermal Analysis and Calorimetry, **74**, 503, 2003.
4. A. V. Slack and G. A. Hollinden, "Sulfur Dioxide Removal from Waste Gases", Noya Data Corporation, NJ, 1975.
5. V. M. Malhotra, P. S. Valimbe, and M. Wright, Fuel, **81**, 235, 2002.

DISCLAIMER STATEMENT

This report was prepared by Vivak Malhotra, Southern Illinois University-Carbondale, with support, in part, by grants made possible by the Illinois Department of Commerce and Economic Opportunity through the Office of Coal Development and the Illinois Clean Coal Institute. Neither Vivak Malhotra and Southern Illinois University-Carbondale, nor any of its subcontractors, nor the Illinois Department of Commerce and Economic Opportunity, Office of Coal Development, the Illinois Clean Coal Institute, nor any person acting on behalf of either:

(A) Makes any warranty of representation, express or implied, with respect to the accuracy, completeness, or usefulness of the information contained in this report, or that the use of any information, apparatus, method, or process disclosed in this report may not infringe privately-owned rights; or

(B) Assumes any liabilities with respect to the use of, or for damages resulting from the use of, any information, apparatus, method or process disclosed in this report.
Reference herein to any specific commercial product, process, or service by trade name, trademark, manufacturer, or otherwise, does not necessarily constitute or imply its endorsement, recommendation, or favoring; nor do the views and opinions of authors expressed herein necessarily state or reflect those of the Illinois Department of Commerce and Economic Opportunity, Office of Coal Development, or the Illinois Clean Coal Institute.

Notice to Journalists and Publishers: If you borrow information from any part of this report, you must include a statement about the state of Illinois' support of the project.